Computational Materials Science 138 (2017) 213–218

Contents lists available at ScienceDirect

Computational Materials Science

journal homepage: www.elsevier.com/locate/commatsci

Excitonic effects on the optical response of monolayer and bilayer graphene-like silicon carbide

You-Zhao Lan

Institute of Physical Chemistry, College of Chemistry and Life Sciences, Zhejiang Normal University, Jinhua 321004, Zhejiang, China

ARTICLE INFO

Article history:
Received 11 May 2017
Received in revised form 26 June 2017
Accepted 28 June 2017

Keywords:
Excitonic effects
Linear optical response
Graphene-like silicon carbide
Interlayer $\pi \rightarrow \pi^*$ transition

ABSTRACT

The graphene-like silicon carbide (SiC) has attracted much attention recently owing to its potential application in optoelectric devices. In this work, we have theoretically investigated the excitonic effects on the dielectric constants [$\varepsilon(\omega)$] of monolayer (ML-) and bilayer (BL-) SiC using the first principle calculations with solving the Bethe-Salpeter equation. The Tran-Blaha modified Becke-Johnson exchange potential combined with the Perdew and Wang correlation potential is used to overcome the underestimate of bandgap. Within the independent particle approximation, BL-SiC not only has the same *intralayer* $\pi \rightarrow \pi^*$ transition in the transverse $\varepsilon(\omega)$ as ML-SiC but also has an *interlayer* $\pi \rightarrow \pi^*$ transition in the longitudinal $\varepsilon(\omega)$. The excitonic effects dramatically change the absorption spectra of two polarization directions (transverse and longitudinal). For the transverse $\varepsilon(\omega)$, BL-SiC has a similar excitonic absorption profile to ML-SiC but shows a blue-shift relative to ML-SiC and an apparent decrease in the binding energy of bright exciton. For the longitudinal $\varepsilon(\omega)$, ML-SiC has a bright exciton with a large binding energy of 1.87 eV related to the $\sigma \rightarrow \pi^*$ transition band, and BL-SiC has a bright exciton with a small binding energy of 0.41 eV related to the *interlayer* $\pi \rightarrow \pi^*$ transition.

1. Introduction

The two-dimensional graphene-like silicon carbide has attracted much attention owing to its different electronic properties from graphene. It is well known that the monolayer graphene exhibits a zero bandgap and has unusual two-dimensional Dirac-like electronic excitations [1]. However, the monolayer SiC (ML-SiC) has a large direct bandgap of 2.54 eV based on the density functional theory (DFT) calculations [2–4] of both the local density approximation (LDA) and the generalized gradient approximation (GGA). Within the many-body *GW* approximation [5], the bandgap of ML-SiC will increase to about 4.0 eV (Ref. [6–10]). ML-SiC would be suitable for applications in optoelectric devices such as light emitting diodes and solar cells owing to its having a direct bandgap. However, isolating the ML-SiC is difficult in practical experiments, and up to now, only ultrathin two-dimensional SiC flakes with a thickness of 0.5–1.5 nm have been obtained [11]; thus, it is important to theoretically characterize the few-layer SiC (FL-SiC).

It has been also shown that the few layer graphene exhibit the notable electronic and optical properties. The bilayer graphene has a tunable bandgap in the range of 70–250 meV with the external electric field applied perpendicular to the bilayer plane [12,13]. In infrared conductivity measurements [14], the principal transitions exhibit a systematic energy-scaling behavior with the number of layers (N) increasing from 1 to 8. The trilayer graphene with *ABA*- and *ABC*-stacking possesses the stacking-order dependent transport properties [15]. The interlayer oriented misalignment [16] leads to dramatically different electronic and optical properties, such as energy-renormalization of the low-energy spectra [17] and twist-angle dependent spectra [18], from the monolayer graphene owing to the complicated interaction between the misaligned layers. Undoubtedly, similar effects of the oriented misalignment [16–18], stacking-order [15,19,20], and N-dependence [14,21–23] on the electronic and optical properties will occur for FL-SiC. The *ABA*-stacked FL-SiC transforms to the indirect bandgap semiconductor owing to the weak interaction between layers, and the corresponding bandgap is less than that of ML-SiC [3] and gradually decreases with an increase of N. Interestingly, although the *ABA*-stacking [3] leads to a direct-to-indirect bandgap transition from ML-SiC to FL-SiC, the oriented misalignment will induce an indirect-to-direct bandgap transition in the bilayer/trilayer SiC [24]. For graphene and bilayer graphene, excitonic effects dramatically change the optical absorption in the ultraviolet and visible region but not the absorbance in the infrared range [25]. Although geometries of ML-SiC and BL-SiC are very

E-mail address: lyzhao@zjnu.cn

http://dx.doi.org/10.1016/j.commatsci.2017.06.040
0927-0256/

similar to those of graphene and bilayer graphene, they are semiconductor and would have different excitonic effects on the optical response.

In this work, we investigate the excitonic effects on the linear optical response of ML-SiC and BL-SiC. In different strategies from the *GW*-Bethe-Salpeter equation (GW-BSE) approach, we use a density functional overcoming the underestimate of bandgap of solids to calculate the band structure, and then perform the Bethe-Salpeter equation resolution. The physical origin of the linear optical absorption related to the interband transitions is carefully analyzed on the basis of the sum-over-states (SOS) calculations within the independent particle approximation (IPA). The excitonic absorption and the corresponding binding energy of exciton are resolved according to the bandgap corrected band structure and the corresponding IPA spectra.

2. Computational details and formulism

2.1. Geometry

The crystal structure of two-dimensional layered SiC is shown in Fig. 1. For ML-SiC, theoretical researches on its geometry and electronic properties [3,6,11] have shown that it has a planar structure with a D_{3h} symmetry and is a semiconductor with a large gap of about 2.54 eV. For BL-SiC, we consider the *AB*-stacking which has two kinds of stacking configurations; one is a carbon atom opposite a silicon atom, the other is a carbon (silicon) atom opposite a carbon (silicon) atom. According to Kaplan et al. [26], the former configuration is more favorable in energy than the latter one; thus in our present work we only focus on the former configuration (*i.e.*, a carbon atom opposite a silicon atom). We optimized these two structures by using the density functional theory approach within the GGA of the Perdew, Burke, and Ernzerhof (PBE) functional [27], as implemented in the CASTEP code [28]. A *k*-point mesh of $10 \times 10 \times 1$, a force threshold of 0.01 eV/Å, and a stress threshold of 0.02 GPa were used for optimization. The optimized distance between the adjacent layers is 3.73 Å (Fig. 1), in consistent with the experimental determination [11]. A vacuum layer of 15 Å was used to assure a negligible interaction between the slabs. With a relaxation of the unit cell, the optimized lattice lengths ($a = b$) are 3.10 Å (Fig. 1), in agreement with previous theoretical researches [3,6].

2.2. Band structure

The band structure calculations were performed by solving the self-consistent Kohn-Sham equations within the GGA. The highly accurate all-electron full potential linearized augmented plane wave (FP-LAPW) method [29] implemented in ELK code [30] was used. Since the conventional LDA and GGA functionals generally underestimate the bandgap of solids, we used the Tran-Blaha modified Becke-Johnson (mBJ) exchange potential [31] combined with the LDA based Perdew and Wang (PW) correlation potential [32] (mBJ-PW). The use of the mBJ-PW functional gives a good agreement between theoretical and experimental band gaps for a majority of solids [31]. In the use of mBJ-PW functional, there is an important tunable parameter *c* which is defined as [31]:

$$c = \alpha + \beta\left(\frac{1}{V_{cell}}\int_{cell}\frac{|\nabla\rho(r)|}{\rho(r)}d^3r\right)^{1/2} \quad (1)$$

where α and β are two free parameters, V_{cell} is the unit cell volume, and ρ is the electron density. For $c = 1$, we will go back to the original BJ potential [33]. By comparing with both the experimental bandgaps and the theoretical *GW* ones, Tran and Blaha have shown that the optimal *c* value lies in the range of 1.1–1.3 and 1.4–1.7 for solids with small (<1.0 eV) and large (>1.0 eV) bandgaps, respectively. Herein, we decided an optimal *c* value on the basis of the *GW* bandgaps. Table 1 lists the bandgaps of ML-SiC based on different GGA and *GW* calculations. For ML-SiC, the PBE bandgap is a direct gap of 2.57 eV while the *GW* bandgap ranges from 3.80 to 4.40 eV depending on different *GW* approximations. On the basis of the *GW* bandgaps, we obtain an optimal *c* value of 1.5 which leads to an indirect mBJ-PW bandgap of 3.93 eV for ML-SiC. This optimal *c* value was also used to calculate the bandgaps of BL-SiC because it has a similar band structure to ML-SiC [3]. Note that for ML-SiC, the LDA and PBE calculations separately yield the indirect (K-M) and direct (K-K) bandgaps [3,6,9], and similar cases occurs for the GW calculations based on different plasmon-pole models or approximation levels used [6–10]. Actually, the bottom of the conduction band at the K point is very close to that at the M point and the corresponding energy difference is only 0.05 eV. In our mBJ-PW calculation, the K-M and K-K gaps are 3.91 and 4.08 eV, respectively. For BL-SiC, our mBJ-PW calculations show that it has an indirect bandgap, similar to the PBE calculation [3]. In our present work, we only consider the vertical transitions. The band structure calculations were preformed with a dense *k*-point mesh of $60 \times 60 \times 1$ to assure the converged energy.

Table 1
Bandgaps (eV) of ML-SiC and BL-SiC based on different theoretical calculations.

Methods	ML-SiC	BL-SiC
PBE	2.57	2.20
mBJ-PW	3.93	3.47
GW[a]	4.19[b], 4.42[c], 3.88[d],3.96[e], 3.90[f]	

[a] For ML-SiC only.
[b] Reference [6] GW^0 ($12 \times 12 \times 1$ k-point mesh).
[c] Reference [9] G^0W^0 ($18 \times 18 \times 1$ k-point mesh).
[d] Reference [10] G^0W^0.
[e] Reference [7] G^0W^0.
[f] Reference [8] GW^0.

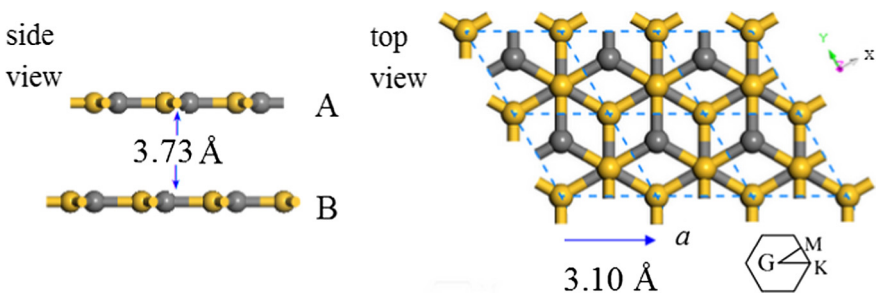

Fig. 1. Crystal structures of ML-SiC and BL-SiC. The Cartesian coordinate system (top right) is for the top viewed structure. The hexagonal lattice length (a = b) and interlayer distance are 3.10 and 3.73 Å, respectively. The unit cells are indicated by the dashed boxes.